Na2HPO4-modified NaY nanocrystallites: Efficient catalyst for acrylic acid production through lactic acid dehydration

Journal:	*Catalysis Science & Technology*
Manuscript ID:	CY-ART-11-2013-000935.R1
Article Type:	Paper
Date Submitted by the Author:	19-Jan-2014

Complete List of Authors:	Zhang, Junfeng; Nanjing University, Chemistry Department Zhao, Yuling; Nanjing University, Chemistry Department Feng, Xinzhen; Nanjing University, Chemistry Department Pan, Min; Nanjing University, Chemistry Department Zhao, Jing; Nanjing University, Chemistry Department Ji, Weijie; Nanjing University, Au, Chak-tong; Hong Kong Baptist University, Chemistry

Catalysis
Science & Technology

Cite this: DOI: 10.1039/c0xx00000x

PAPER

www.rsc.org/xxxxxx

Na_2HPO_4-modified NaY nanocrystallites: Efficient catalyst for acrylic acid production through lactic acid dehydration

Junfeng Zhang,[a] Yuling Zhao,[a] Xinzhen Feng,[a] Min Pan,[a] Jing Zhao,[a] Weijie Ji, [a,] * and Chek-Tong Au [b,] *

Received (in XXX, XXX) Xth XXXXXXXXX 20XX, Accepted Xth XXXXXXXXX 20XX

DOI: 10.1039/b000000x

By regulating the H_2O/SiO_2 molar ratio (n =13.8, 16.9, 20.1, 26.3), NaY zeolites of different particle sizes (NaY-*n*, 50-400 nm) were synthesized, and the NaY-*n* was modified with disodium hydrogen phosphate, Na_2HPO_4. The as-prepared catalysts are highly effective for the dehydration of sustainable lactic acid (LA) to produce acrylic acid (AA). Through the optimization of NaY particle size and Na_2HPO_4 loading, AA yield as high as 74.3% can be achieved under mild condition (340°C). In terms of employed feed rate of lactic acid and amount of catalyst, the AA formation rate is 12.0 mmol g_{cat}^{-1} h^{-1}, the highest one ever reported for LA dehydration to AA. Employing slightly low Si/Al ratio in NaY-*n* can modify catalyst acidity, while the pre-applied Na^+ ion-exchange and the following Na_2HPO_4 loading can effectively reduce the number of acid sites, particularly the Brønsted ones on NaY-*n*. Equrally important structural features of NaY-*n* are their shorter pore channels (or even incompletely developed zeolite texture) and relatively larger $S_{external}/S_{BET}$ ratio, which favors quick product departure from catalyst surface, and reduces the possiblity of side reactions occuring inside the long channels. Appropriate surface acidity together with unique structural feature of NaY-*n* ensures efficient LA conversion with high dehydration selectivity. Higher surface concentration of Na^+ on Na_2HPO_4/NaY-*n* also favors sodium lactate meanwhile suppresses poly-lactate as well as inactive carbon formation, coorsponding to the superior performance as well as improved durability of Na_2HPO_4/NaY-*n*.

.

1. Introduction

Acrylic acid (AA) is a highly demanded raw material, and industrially it is produced through the oxidation of propylene originated from non-renewable petroleum. The direct fermentation of biomass (such as sugar) to AA was under investigation [1]. Straathof et al. [2] analyzed the metabolic process of biomass to AA and figured out three major pathways that were involved in AA generation. With the prospect of Lactic acid (LA) being derived from sustainable biomass, the catalytic dehydration of LA becomes an attractive option for AA production. [3] LA has bi-functional groups (-OH and –COOH), it can be produced through chemical synthesis and biomass-based fermentation processes [4] with the latter being conducted for many years. [5] Recently John et al. [6] and Dusselier et al. [7] made thorough overviews on the feasibility of using LA as raw resource for petrochemical production, and commented on the related economical prospects and the economic effectiveness of the fermentation technology in the exploration as well as exploitation of biomass materials for LA production. On the other hand, chemical production of LA and other value-added substances using renewable feedstocks have been emphasized and explored.[8] Holm et al.[8b,8d] reported a catalytic process for direct formation of methyl lactate from common sugars over Lewis acidic zeotypes such as Sn-Beta at 160 °C. With sucrose as substrate, the yield of methyl lactate can be as high as 68%, and the catalyst can be easily recovered by filtration and reused multiple times after calcination without any substantial change in product selectivity.

As for chemcatalysis production of AA, Holmen et al.[9] observed 68% AA selectivity at LA conversion of >70% over calcined phosphates and/or sulfates. The study of Paparizos et al.[10] on LA dehydration over aluminum phosphate that was treated with inorganic base, and the study of Sawicki et al.[11] on LA dehydration over silica- and alumina-supported phosphate catalysts showed AA yield of ca. 50%. In the mechanistic study of LA conversion to AA over alkali metal nitrate and phosphate, Gunter and coworkers[12] detected lactate species that were formed due to LA-catalyst interaction. They noted that although phosphorus did not promote the target reaction, its presence suppressed side reactions, especially the formation of acetaldehyde; also, AA formation was enhanced because the carboxyl groups were stabilized by the generated phosphate of cyclic structure. The role of phosphorus in stabilizing carboxyl groups was noted previously by researchers such as Monma,[13] Daniel,[14] Watkins [15] and Lee et al.[16] Ghantani et al. [17a] also found that calcium lactate can be formed during dehydration of LA over the calcium hydroxyapatite catalyst and the generated lactate species showed postive effect on protecion of carboxyllic group according to the proposed dehydration mechanism. Peng et al.[17b] reported AA selectivity of 74% at LA conversion of 99.8% over barium sulfate as catalyst, and improved stability was also observed.

Over sodium dihydrogen phosphate (NaH_2PO_4) that was supported on silica, Zhang et al. [18] observed the formation of methyl acrylate (MA) and AA, and “MA+AA” selectivity was approximately 50%, corresponding to LA conversion of 99.5%.

They found that with increase of Na/P ratio, the amount of terminal POH group and surface acidity declined, resulting in higher "MA+AA" selectivity. Furthermore, AA could be produced from LA in a medium of supercritical water containing phosphate or strong base as reported by Lira and McCrackin. [19] However, the reaction conditions were severe and the kinetics was found to be complicated.

Zeolites are solid acids effective for the catalytic dehydration of alcohol and hydroxy-carboxylate acid/ester. [20] It is believed that due to enrichment of reactant(s) in the channels of zeolites, there is enhancement of reactivity. The FAU topology and supercage structure of NaY zeolite are beneficial for molecule accessibility and diffusion, showing high selectivity to small molecule product(s). [21] Compared to the NaY-supported phosphate catalyst, we found that the counterpart using SBA-15 as support showed considerably higher selectivity to 2,3-pentanedione (rather than to AA). [22] Therefore, porous property of catalyst is important to determine AA or 2,3-pentanedione selectivity, particularly when LA dehydration was operated at lower reaction temperature. Moreover, according to Balkus et al.,[23] there is no need for zeolite catalysts to be strong in acidity for LA dehydration. Wang et al. [24] and Sun et al. [25] adopted NaY exchanged with ions of rare earth metals as catalysts. They found that ion exchange at specific position of NaY may induce distortion of crystal cell and consequently a remarkable increase in AA selectivity.

In a previous study, [26] we found that NaY modified with alkali metal phosphates showed 58% AA yield in LA dehydration. Among the modified NaY catalysts, the one modified with disodium hydrogen phosphate (Na_2HPO_4) showed the best performance under optimized conditions. It was found that LA conversion was generally below 80% while AA selectivity over 70%. Therefore, there is room for conversion enhancement with AA selectivity being retained at high level. Compared to the zeolite crystallites that are commercially available, the zeolite crystallites fabricated with smaller size are superior in terms of external surface area, density of specific acid sites, and diffusion path length. [27] The objective of the present study was to develop catalysts that were based on nanosized NaY zeolites. We systematically synthesized NaY nanoparticles of different sizes (50-400 nm) and adopted them to disperse Na_2HPO_4. It was found that the obtained catalysts significantly outperformed the previously reported ones that were supported on commercial NaY. In addition to improvement in overall stability, the new catalyst showed AA yield of 74%, ca. 17% higher than the one that was based on commercial NaY. The AA formation rate is 12.0 mmol g_{cat}^{-1} h^{-1}, which is in fact the highest value ever reported, and can be considered as a significant progress in AA production through the catalytic dehydration of LA. Based on the results of systematic characterization, we discussed in detail the origin of catalyst supremacy as well as the reasons for the difference in characteristics and stability between the commercial NaY-based and nanosize NaY-based catalysts. To help in comparing the important findings of ctalyst design for AA fehydration, Table S1 (ESI) is presented, in which the representative catalyst systems, their performances, and the related operation conditions are summarized.

2. Experimental Section

2.1 Catalyst preparation

NaY_{com} was purchased from the Zeolite Manufactory of Nankai University (China). Nanosize NaY crystallites were synthesized according to a two-stage variable-temperature program without the use of any organic templates, one similar to that described by Fang et al.,[35] Sang et al.,[36] and Valtchev and Bozhilov.[37] The particle size was controlled by regulating the molar ratio of water to SiO_2 (n = H_2O/SiO_2) in preparation. The nominal H_2O/SiO_2 (n) was 13.8, 16.9, 20.1 and 26.3, and the NaY samples are denoted as NaY-n hereinafter. Tipically, 9.46 g of sodium hydroxide (NaOH) was added into desired amount of water. After complete dissolution of NaOH, 5.00 g of aluminum isopropoxide (Chengdu Kelong Chemical Co., Ltd, China) was added under agitation for 2 h. Simutanueously, 35.25 g of colloidal SiO_2 solution (30wt%, Adrich) was slowly added into the above mentioned sodium aluminate solution under vigorous stirring for 15 min. The resulting solution was aged at 25 °C for 24 h under stiring, subsequently tranferred into autoclave and aged for additional 24 h at 38 °C. Finally, the precursor gel was hydrothermally treated at 60 °C for 48 h. The resulting suspension was filtrated, and the collected solids were dried at 80 °C. The Na^+ ion-exchange pretreament of NaY_{com} and NaY-n was conducted as following: the weighted NaY sample was added into an aqueous $NaNO_3$ solution (1 mol/L) with a solid/liquid ratio being 1:10 (w/w) and the suspension was stirred at 70 °C for 6 h. After that the solids were collected by filtration, washed with water repeatedly to remove the residual Na^+ ions. The material was then dried at 110 °C overnight. The Na_2HPO_4 was introduced to NaY-n through impregnation. Typically, NaY-n of 2.5 g was added into 25 ml aqueous Na_2HPO_4 solution (0.096 mol/L). The resulting suspension was stirred at 40°C for 4 h, and the slurry was dried under vacuum (in a rotary evaporator) and further dried at 120 °C overnight. The obtained catalyst (denoted as Na_2HPO_4/ NaY-n hereinafter) was pressed and crushed into 40-60 mesh particles. As a reference, a Na_2HPO_4/NaY_{com} catalyst using commercially available NaY (denoted as $NaY_{com)}$ as support was also fabricated in a similar manner. The Na_2HPO_4 loading of the catalysts was 12 wt% unless specified otherwise.

2.2 Catalyst activity

All reactions were carried out at atmospheric pressure in a vertical fix-bed quartz reactor 8 mm in internal diameter and 500 mm in length. The catalyst (1.5 g) was placed in the middle and the upper part of the reactor was filled with quartz chips for preheating the LA feedstock which was introduced by a syringe pump using N_2 as carrier gas (30 ml/min). Before the start of reaction, the catalyst was heated at a rate of 10°C/min to a designated temperature in N_2 and kept at this temperature for 3 h. Then an aqueous solution of LA (34 wt%) was introduced at a rate of 6 ml/h, and the products were collected in a cold trap during a reaction period of 2 h and analyzed using a gas chromatograph equipped with FID and HP-FFAP capillary column using valeric acid as internal standard. LA conversion, AA yield and selectivity were reported as percentage of theoretical molar yield based on the amount of LA that was fed into the reactor.[38] Repeated measurements were performed to

assure reproducibility of results. The data shown in the present study are averaged values with deviations of ±2%.

2.3 Catalyst characterization

Powder X-ray diffraction of as-synthesized and Na_2HPO_4-modified NaY nano-crystallites was conducted on a Shimadzu XRD-6000 diffractometer with Cu-Kα radiation (operated at 40 kV and 40 mA) at a scanning speed of 5°/min in the 5-70°(2θ) range. Scanning electron microscopic (SEM) images of samples were taken on an S-4800 SEM instrument. The elemental composition of samples was checked by X-ray fluorescence analysis over an ARL-9800 spectrometer. X-ray photoelectron spectroscopic (XPS) measurement was performed on a PHI5000 VersaProbe instrument with Al Kα radiation. The binding energy (BE) was calibrated against the C1s signal (284.6 eV) of contaminant carbon. Elemental surface composition was estimated on the basis of peak areas which were normalized using Wagner factors. Ammonia temperature-programmed desorption (NH_3-TPD) was conducted to measure the surface acidity of catalysts. The signal of NH_3 was measured by a thermal conductivity detector (TCD). Catalyst of 0.1 g was first heated in an Ar flow (30 ml/min) to 400 °C and kept at this temperature for 1 h. Then the sample was cooled to 100 °C in flowing Ar. After that, NH_3 adsorption was performed at 100 °C for 1 h. Finally, NH_3-TPD was carried out in a He flow (30 ml/min) with the sample being heated to 500 °C at a rate of 10 °C /min. The FTIR spectra of pyridine adsorption were recorded in the range of 1000-4000 cm^{-1} on a Bruker VERTEX70 spectrometer. The samples were pressed into self-supporting wafers containing 10 mg of material, and then the wafers were mounted inside a Pyrex vacuum cell and degassed at 400 °C for 2 h. Samples were allowed to cool down to room temperature (RT), and pyridine vapor was admitted into the cell and adsorption lasted for 1 h. Subsequently, the samples were heated up to 200 °C under vacuum and kept at this temperature for 2 h then cooled down to RT for spectrum recording. The specific surface area and pore volume of catalysts were measured by N_2 adsorption at 77 K on a Micrometrics ASAP 2020 instrument. Prior to N_2 adsorption, the samples were treated under vacuum at 350 °C for 8 h. The specific surface areas were estimated using the BET method, while the pore volumes were calculated by the t-plot method.

3. Results and discussion

3.1 Characterization of fresh catalysts

XRD Fig.1a shows the XRD patterns of NaY-*n* which are typical of FAU-type zeolite. According to the results of Huang et al.[27,35], the size of NaY crystallites can be reflected by the width and height of diffraction peaks. One can see that crystallinity enhances with rise of *n* (*n* = 13.8, 16.9, 20.1, 26.0), suggesting that the formation of NaY crystallites is favourable at a higher content of water in the gel precursor. There are other small peaks observed over NaY-*13.8* and NaY-*16.9* as compared to NaY-*26.3*, suggesting that it is possible to have minor non-zeolite structure in the cases of NaY-*13.8* and NaY-*16.9*. Note that the H_2O/SiO_2 ratio adopted for the generation of NaY-*13.8* and NaY-*16.9* was relatively low, and the decline of water content might result in lower uniformity of suspension during preparation. As a result, the as-obtained samples were poor in zeolite structure and crystallinity. The Na_2HPO_4/NaY-*n* catalysts essentially retain the FAU structure (Fig.1b). Note that the diffraction peak at 2θ = 6.2° corresponding to (111) reflection significantly diminishes after Na_2HPO_4 modification. The phenomenon suggests that despite there is no obvious change in phase structure, there is a certain change in NaY morphology as reported previously by us.[26] In addition, since there is no XRD signal ascribable to Na_2HPO_4 species, we deduce that the dispersion of Na_2HPO_4 is high.

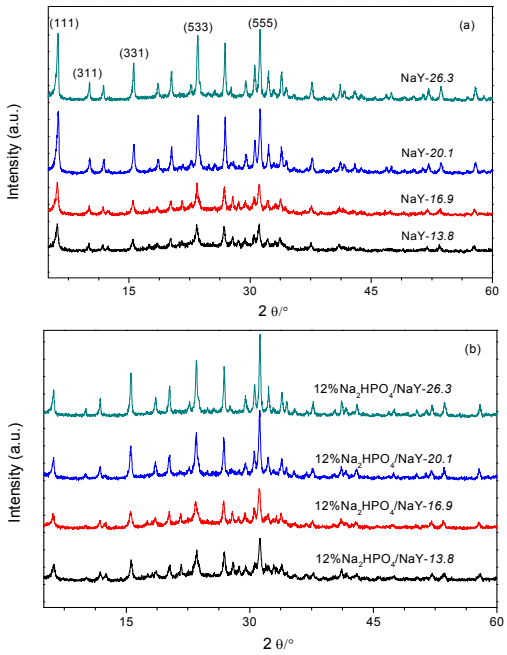

Fig. 1. XRD patterns of (a) NaY-*n* and (b) Na_2HPO_4/NaY-*n*.

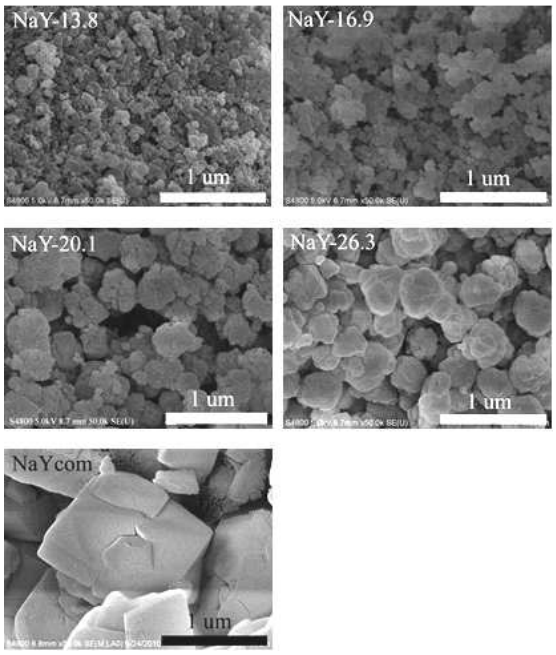

Fig 2. SEM images (a-e) of NaY-*n* and NaY_{com}.

SEM Shown in Fig. 2 are the SEM images of NaY-*n* and NaY_{com}. The NaY-*n* samples (Figs. 2a-d) are uniform in size distribution. The size of primary particles increases from approximately 50 to 400 nm with increasing *n* values; a phenomenon of this kind was also reported by Song et al. [28] The size of NaY_{com} crystallites is 1.5-2 μm, roughly ten times bigger than that of NaY-*n*. Moreover, there is morphological difference between the two: NaY-*n* are with round edges while NaY_{com} with square edges. The important structural features of NaY-*n* are their shorter pore channels (or even not well-developed zeolite texture as in the cases of NaY-*13.8* and NaY-*16.9* as revealed in Fig. 1) and relatively larger external surface area (Table 1), which can favor quick product departure from catalyst surface, and reduce the possiblity of side reactions occuring inside the long channels.

N_2 sorption The size and pore volume of samples are commonly measured based on sorption isotherms of N_2 condensation at 77 K;[29] and the BET surface areas (S_{BET}) of microporous samples can be obtained as well. However, one should bear in mind that there are limitation in BET measurement of microporous adsorbents [30] and S_{BET} can only be compared in empirical values among the same kind of porous materials.[31] The characteristics of NaY-*n* and NaY_{com} without and with Na_2HPO_4 loading are listed in Table 1. With rise of *n* from 13.8 to 26.3, the surface area of NaY-*n* increases from 418 to 642 m^2/g. The observation is consistent with that reported by Huang et al.[27] It is thought that the BET surface area is related to the crystallinity of NaY-*n*. Comparatively low crystallinity of NaY-*n* (especially NaY-*13.8*) corresponds to incompletely developed micropores and thus to smaller in specific surface area as well as in micro-porous volume (Table 1). On the other hand, the well growth of primary particles and high crystallinity of NaY_{com} (as revealed in SEM image) can account for its large specific surface area. Due to the undeveloped micropore/texture of nanosized NaY-*n* to certain degree (especially in the case of NaY-*13.8*), the contribution of micropores to surface area and V_{total} decreases (Table 1). However, it is actually not a disadvantage, since the deep pores inside the zeolite crystallites can cause a notable diffusion issue, which in turn inevitably facilities side reactions. In addition, stacking of nanosized NaY-*n* could also develop certain mesopores (Fig. S1) which contribute notably to V_{total} but insignificantly to S_{BET}. The overall effect is that surface area decreases notably while V_{total} declines slowly on the sample serial from NaY_{com} to NaY-*13.8*.

In a previous study,[26] we found that the introduction of Na_2HPO_4 to the commerical NaY zeolite led to decrease of S_{BET} and pore volumes (V_{total} and V_{micro}). The similar observations were made on NaY-*n* of the present study. With the introduction of Na_2HPO_4, there would be plugging of pores, especially so when micropore volume (V_{micro}) and specific surface area (S_{BET}) are getting smaller. The ratio $S_{external}$ to S_{BET} for all of the samples has been included in Table 1. The $S_{external}/S_{BET}$ ratio of NaY-*26.3* is only slightly larger than that of NaY_{com}. We thought that the crystallinity of NaY-*26.3* is close to that of NaY_{com}, but the porosity of the two samples is somehow different, which is reflected in the values of S_{BET}, V_{total}, and V_{micro} of the two samples. The results of NaY-16.9 were also included in Table 1. Note that Na_2HPO_4/NaY-*n* in smallest particle size showed the highest $S_{external}/S_{BET}$ ratio. This is one of critical factors in determining catalytic behavior of LA dehydration. In the NaY-*n* serial samples, the highest $S_{external}/S_{BET}$ ratio is observed on NaY-*20.1*, which suggests that the $S_{external}/S_{BET}$ ratio is determined by not only the particle size, but also the developed zeolite texture.

Table 1. Characteristics of NaY-*n* and NaY_{com}

Sample	Si/Al	Na/Al	S_{BET} (m^2/g)	V_{total} (cm^3/g)	S_{ex} (m^2/g)	V_{micro} (cm^3/g)	S_{ex}/S_{BET}
NaY_{com}	2.46	0.96	686	0.37	81	0.26	0.12
NaY-*26.3*	1.56	0.97	642	0.38	85	0.24	0.13
NaY-*20.1*	1.58	0.98	513	0.38	102	0.25	0.20
NaY-*16.9*	1.58	0.98	504	0.33	95	0.22	0.19
NaY-*13.8*	/	/	418	0.25	73	0.11	0.18
loaded NaY_{com}	2.6	1.43	391	0.23	32	0.12	0.08
loaded NaY-*26.3*	1.60	1.29	405	0.21	29	0.18	0.07
loaded NaY-*20.1*	1.61	1.28	372	0.23	48	0.14	0.13
loaded NaY-*16.9*	1.61	1.29	288	0.24	50	0.11	0.17
loaded NaY-*13.8*	/	/	182	0.19	43	0.065	0.24

NH_3-TPD The NH_3-TPD study can provide information related to overall acidity as well as strength of acid sites. Shown in Fig. 3 are the NH_3-TPD profiles obtained over the NaY-*n*, NaY_{com}, Na_2HPO_4/NaY-*n*, and Na_2HPO_4/NaY_{com} samples. Over NaY-*n* and NaY_{com} before and after Na_2HPO_4 addition, there are weak, medium, and medium strong acid sites corresponding to NH_3-desorption in the 150-200 °C, 200-260 °C, and 260-400 °C ranges, respectively. The NaY-*n* samples show slightly higher acid strength than NaY_{com} in view of the NH_3-desorption temperatures (Fig. 3a). Compared to NaY-*n*, NaY_{com} has lower fraction of sites that are medium strong in acidity, this is understandable since the Si/Al ratio of NaY-*n* is relatively higher (Table 1). Across the NaY-*n* samples, there is a tendency that surface acidity declines with increasing *n* value; on the other hand, the fraction of medium strong acid sites increases with increasing *n* (i.e. increasing particle size). This is plausibly due to slight decrease in Si/Al ratio [27] as well as enhancement of NaY phase purity and crystallinity. With the introduction of Na_2HPO_4, the number of acid sites of these three kinds decreases notably with no obvious change in acid strength (Fig. 3b).

The overall acidity of different samples was quantified based on the area of NH_3 desorption peaks in the TPD profiles, and the results are shown in Table S2 (ESI). A general picture is that the overall acidity decreases after Na_2HPO_4 modification. However, it is rather complicated to individually compare the acidity among the unmodified and Na_2HPO_4 modified NaY samples, this is because the fractions of medium strong, medium, and weak acid sites seem to change obviously from one to another, and reliable quantification of medium strong, medium, and weak acid sites is practically difficult due to severe overlap of the corresponding peaks/shoulders. Nevertheless, the overall acidity of the loaded NaY-*n* and NaY_{com} is close each other except for the loaded NaY-*26.3*, but qualitatively, the fraction of medium strong acid sites over the Na_2HPO_4 modified NaY-*16.9*, NaY-*20.1*, and NaY-*26.3* appears relatively higher than that on the Na_2HPO_4 modified NaY_{com} as well as NaY-*13.8*, which may be in part responsible

for their catalytic behaviors. Note that although the Si/Al ratio apparently influenced the catalytic behavior of various catalysts, the catalyst nature is actually multi-affected by Si/Ai ratio, synthetic condition, and resulting structure in the current study.

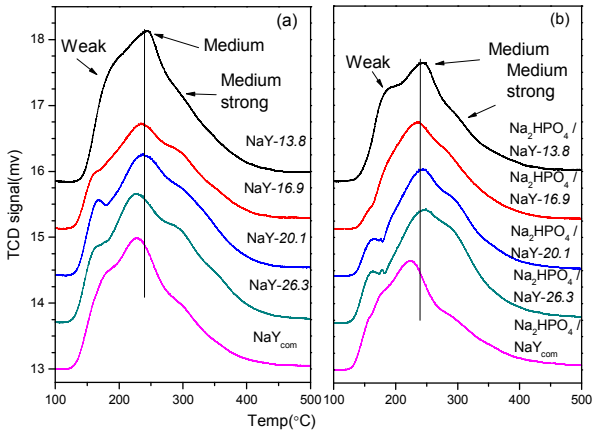

Fig. 3. NH_3-TPD profiles collected over (a) unmodified NaY and (b) 12%Na_2HPO_4-modified NaY.

Pyridine-adsorption FTIR FTIR spectra of pyridine adsorption on NaY-*n* and Na_2HPO_4/NaY-*n* are shown in Fig. 4. The 1545 and 1450 cm^{-1} bands are attributed to pyridine adsorption on Brønsted acid sites (pyridinium ion) and Lewis acid sites (i.e. accessible Al^{3+} or Na^+ sites), respectively. [32] As for the 1490 cm^{-1} band, it is believed to be a co-contribution of pyridine adsorption on Lewis as well as on Brønsted acid sites. [33] From Fig. 4a, it is clear that both Brønsted and Lewis acid sites exist on NaY-*n* and NaY$_{com}$. The amount of Brønsted acid sites can be affected by both the Si/Al ratio of zeolite sample and the efficiency of Na^+ ion-exchange pre-treatment. The Si/Al ratio of NaY-*n* is somewhat lower than that of NaY$_{com}$ (Table 1), meanwhile the fraction of Brønsted acid sites of NaY-*n* is also higher than that of NaY$_{com}$ (Fig. 4).

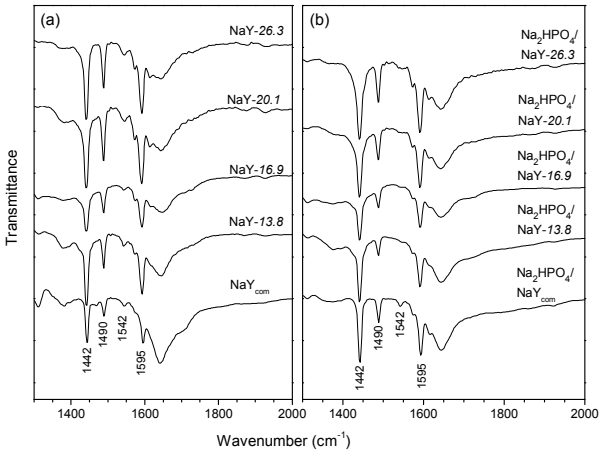

Fig. 4. FTIR spectra of pyridine adsorption collected over (a) unmodified NaY, and (b) 12%Na_2HPO_4-modified NaY.

On the other hand, the XRF measurements of NaY$_{com}$ and NaY-*n* reveal that the Na/Al ratio of NaY$_{com}$ is smaller than that of NaY-*n* (Table 1), therefore, it is plausible that in the case of NaY-*n*, higher fraction of protons is substituted by Na^+ ions during the Na^+ ion-exchange pre-treatment. When Na_2HPO_4 is introduced to NaY-*n*, there is diminution of pyridine adsorption peaks at ca. 1542 cm^{-1} (Fig. 4b), indicating the elimination of Brønsted acid sites, but this is not the case for NaY$_{com}$. According to the experimental setup, the samples after pyridine adsorption were heated up to 200 °C and degased under vacuum for 2 h. It is difficult, however, to remove hydrogen bonded pyridine species which result in the peaks at 1595 cm^{-1}. [32] Employing slightly low Si/Al ratio in NaY-*n* synthesis can modify catalyst acidity, while the pre-applied Na^+ ion-exchange and the following Na_2HPO_4 loading can effectively reduce the number of acid sites, particularly the Brønsted ones on NaY-*n*. Appropriate surface acidity together with unique structural feature of NaY-*n* ensures efficient LA conversion with high dehydration selectivity.

3.2 Catalyst activity

It was observed in our previous study that with the optimization of reaction conditions (reaction temperature, LHSV, LA concentration), the Na_2HPO_4/NaY$_{com}$ catalyst showed good performance in LA dehydration to AA (~58% AA yield).[26] In the present study, the Na_2HPO_4/NaY-*n* catalysts were evaluated under similar reaction conditions, and the results are illustrated in Fig. 5 and Table 2.

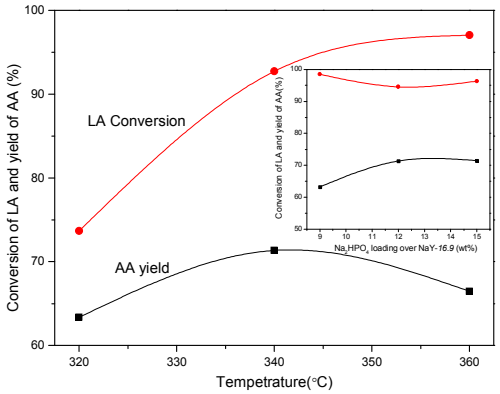

Fig. 5. Temperature dependence of LA conversion and AA yield observed over 12%Na_2HPO_4/NaY-*16.9*. The effect of Na_2HPO_4 loading on LA conversion and AA yield at 340 ºC is also illustrated in the inset.

As shown in Fig. 5, LA conversion over 12%Na_2HPO_4/NaY-*16.9* increases from 75.5% to 98.9% as reaction temperature is raised from 320 to 360 °C, while AA yield first increases with temperature rise from 320 to 340°C and then declines above 360°C. An AA yield of 71.3% can be obtained in a single-pass reaction at 340 °C. Note that temperature rise in the 320-340°C range has caused enhancement in LA conversion, while in the 340-360 °C range a rise in temperature has little impact on LA conversion but considerable enhancement of side reactions (generating acetaldehyde and acetic acid, causing reduction in AA selectivity). As illustrated in the inset (Fig. 5), Na_2HPO_4 loading also affects AA yield. Over 9%Na_2HPO_4/NaY-*16.9* and

15%Na_2HPO_4/NaY-*16.9*, AA yields are 63.2% and 71.4%, respectively, while there is only slight change in LA conversion. It was found that the optimal Na_2HPO_4 loading on NaY-16.9 is 12% by weight.

Shown in Table 2 are the performances of NaY-*n* and NaY_{com} as well as those of Na_2HPO_4/NaY-*n* and Na_2HPO_4/NaY_{com} with 12% loading. Clearly, NaY-*n* (*n* = 13.8, 16.9, 20.1, 26.3) outperform NaY_{com}. In general, NaY_{com} shows higher LA conversion while NaY-*n* higher AA selectivity. In our experiment, The Na^+ content in NaY-*n* (detected by XRF and XPS, not shown) is higher than that in NaY_{com}. According to Gunter and co-workers,[12a,12c] ample provision of Na^+ ions is a beneficial factor because the formation of AA involves the generation of sodium lactate through a step of proton transfer from LA. It is suggested that higher concentration of surface sodium lactate species accounts for higher AA yield.

Table 2. Yield of certain products, LA conversion and AA selectivity observed over NaY-*n* and 12%Na_2HPO_4/NaY [a]

Catalysts	Yield of certain products (%)				LA Conv. (%)	AA Sel. (%)
	Acetaldehyde	2,3-pentanedione	Propanic acid	AA		
NaY_{com}	22.0	3.1	1.6	35.5	95.5	37.2
NaY-*13.8*	37.7	3.0	0.8	38.9	89.6	43.4
NaY-*16.9*	19.9	3.1	1.3	41.1	88.9	46.2
NaY-*20.1*	13.6	2.5	1.1	42.0	91.6	45.9
NaY-*26.3*	18.4	2.4	1.6	34.0	86.2	39.5
Na_2HPO_4/NaY_{com}	4.6	4.6	1.0	54.0	82.3	65.7
Na_2HPO_4/NaY-*13.8*	4.8	5.3	1.1	70.9	92.3	76.8
Na_2HPO_4/NaY-*16.9*	3.8	5.0	1.1	71.3	94.6	75.4
Na_2HPO_4/NaY-*20.1*	5.1	5.2	1.0	74.3	93.5	79.5
Na_2HPO_4/NaY-*26.3*	4.5	4.4	1.0	70.7	94.3	75.0

[a] Notes: N_2 flow rate = 30 ml/min, LA concentration in liquid feed = 34%, reaction temperature = 340°C. Other products include propanediol, poly-lactate as well as surface carbon species.

With introduction of Na_2HPO_4 to NaY, there is an increase of 6-8% in LA conversion, but an increase of ca. 30% in AA selectivity. The highest AA yield of 74.3% with 79.5% AA selectivity is observed over 12%Na_2HPO_4/NaY-*20.1*. It is noticed that Na_2HPO_4/NaY-*n* showed similar catalytic performances (Table 2). This is understandable because the size of primary zeolite particles of Na_2HPO_4/NaY-*n* is actually comparable within the serial Na_2HPO_4/NaY-*n* although the dimension of the secondary particles becomes larger in the cases of NaY-*20.1* and NaY-*26.3* owing to stacking of primary particles. On the other hand, relatively lower crystallinity (based on XRD result) and less developed NaY zeolite structure (based on N_2 sorption data) in the cases of NaY-*13.8* and NaY-*16.9* may somehow offset the small size effect. In contrast, the higher crystallinity and well developed NaY structure of NaY-*26.3* likely compensate the large size effect. As a consequence, the overall activity of Na_2HPO_4/NaY-*n* is close to that of the individuals. However, it should be emphasized that Na_2HPO_4/NaY-*n* significantly outperform Na_2HPO_4/NaY_{com} (Table 2), which made us to conclude that the small-sized catalysts (50-400 nm) are indeed superior to the large-sized one (~2000 nm). The highest AA formation rate obtained over Na_2HPO_4/NaY-*20.1* (12.0 mmol g_{cat}^{-1} h^{-1}) is approximately 3.9 times as much as that obtained on barium sulphate reported by Peng et al. [17b]

Based on the results of NH_3-TPD and pyridine-adsorption FTIR studies, one can envisage that fine-tuning of NaY acid property by means of Na_2HPO_4 modification is critical for selective production of AA from LA. The results of Balkus et al. [23] and Peng et al. [17b] indicated that strong surface acidity is not essential. The acidity requested for LA dehydration could vary with catalyst nature of different systems. Nevertheless, our studies on the NaY-based catalysts revealed that the weakened surface acidity due to Na^+-ion exchange pretreatment and Na_2HPO_4 modification indeed enhanced AA selectivity. Referring to the results of SEM investigation, one can infer that the nano-scaled NaY zeolites promote the dispersion of Na_2HPO_4 species as well as enhance mass transfer of AA product in the short zeolite channels. In other words, catalyst performance could be somewhat morphology-specific. The size and aggregation state of primary particles have to be optimized so as to achieve crystallinity and texture most suitable for the target reaction. This is evidenced by the results observed over the serial Na_2HPO_4/NaY-*n* samples in terms of variation in acetaldehyde selectivity. With Na_2HPO_4 introduction, acetaldehyde formation is drastically suppressed. On this aspect, the NaY-*n* samples are obviously superior to NaY_{com}. Furthermore, the presence of phosphorus is known to stabilize the carboxyl groups of LA and AA. [13-15] According to the DFT calculation made by Zhang et al. [18] and the study reported by Ghantani et al.,[17a] once the carboxyl group of LA is stabilized by the phosphate species, decarbonylation of LA can be effectively suppressed, which in turn enhances AA selectivity. It is deduced that the mechanism of this study is similar to that proposed by Ghantani et al. expect that the calcium lactate serves as active species in their study is replaced by the NaY-*n* supported sodium lactate in our case.

3.3 XPS measurement of fresh and used catalysts

The surface elemental composition of fresh and used catalysts was examined by XPS technique. As shown in Table 3, the NaY-*20.1* sample has a surface Si/Al ratio of 1.93. With the introduction of Na_2HPO_4, there is decline of Si/Al ratio from 1.93 to 1.8, lower than that of 12%Na_2HPO_4/NaY_{com} (2.7). The results of XRF measurement show that the bulk Si/Al ratio of NaY-*20.1* is somewhat lower than that of NaY_{com}, suggesting that more Na^+ could be introduced to the NaY-*20.1* zeolite through ion-exchange pre-treatment. Moreover, higher dispersion of Na_2HPO_4 has been achieved over NaY-*n* than over NaY_{com}, especially on the external surfaces of NaY-*n*. Therefore, it is reasonable to find that the surface Na^+ concentration of 12%Na_2HPO_4/NaY-*20.1* is higher than that of 12%Na_2HPO_4/NaY_{com}. High surface Na^+ concentration is favorable for developing sodium lactate which is considered as the real active species for LA dehydration to AA.

The Na1s and C1s BEs of catalysts were measured to understand the chemical nature of catalyst surface. Compared

with the Na1s peak of NaY-*20.1* (at 1071.7 eV), that of Na_2HPO_4/NaY-*20.1* shows obvious increase in peak intensity but no shift in peak position (Fig. 6a). In the cases of used Na_2HPO_4/NaY-*20.1* and used Na_2HPO_4/NaY_{com}, there is a shift of Na1s peak position to lower BE, indicating a change in chemical environment of Na^+ and implying the generation of sodium lactate species. In Fig. 6b, one can see that the C1s peak increases in intensity and shifts toward lower BE after reaction, suggesting the deposition of carbon-containing species during the reaction. In addition, new C1s peaks at approximately 287.9 eV ascribable to carbonyl group of sodium lactate [34] are observed over the used catalysts. Thus the XPS investigation provided evidence for the in situ formation of sodium lactate species during the reaction.

On the other hand, there is little change in surface concentration of phosphorus, suggesting that the surface phosphate species are quite stable, providing consistent functionality of stabilizing the carboxyl groups.

Table 3. Surface elemental composition of representative catalysts

Sample	Surface elemental composition (at %)						
	C	Na	Al	Si	O	P	Si/Al
NaY-20.1, fresh	23.7	8.8	6.9	13.3	47.3	/	1.9
Na_2HPO_4/NaY-20.1, fresh	10.9	16.4	5.9	10.8	54.0	2.1	1.8
Na_2HPO_4/NaY-20.1, used	21.4	15.1	4.9	8. 5	47.7	2.4	1.7
Na_2HPO_4/NaY_{com}, fresh	15.1	10.5	5.3	14.5	52.4	2.2	2.7
Na_2HPO_4/NaY_{com}, used	20.2	15.5	4.0	10.0	47.9	2.5	2.5

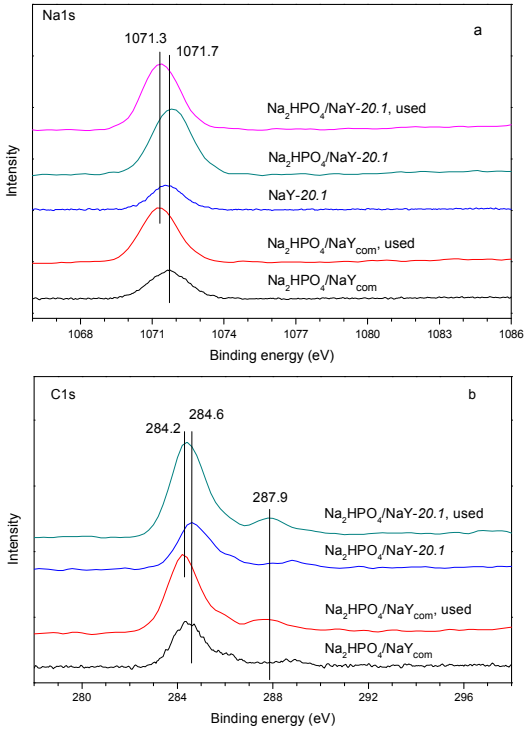

Fig. 6. Na1s and C1s spectra of the fresh and used catalysts.

3.4 FTIR study of fresh and used catalysts

In order to better understand the catalytic process, FTIR technique was applied to examine the fresh and used catalysts and the results are shown in Fig. 7. Over the used catalyst, IR bands at 1411 and 1577 cm^{-1} ascribable to sodium lactate species are detected. Therefore, besides the XPS results, we have IR evidence to support the in situ generation of sodium lactate. Similar observation was reported by Gunter et al.[12d] From Fig. 7, one can see that 12%Na_2HPO_4/NaY-*20.1* has greater amount of sodium lactate species than 12%Na_2HPO_4/NaY_{com}, and the observation is consistent with the XPS results. According to the studies of Gunter and co-workers[12a,12c] and us,[26] the in situ generated sodium lactate entities are responsible for LA dehydration to AA. That Na_2HPO_4/NaY-*20.1* is superior to Na_2HPO_4/NaY_{com} in the target reaction is reflected in the higher concentration of sodium lactate on the surface of the former. On the other hand, the broad band centred at 2972 cm^{-1} can be ascribed to the poly-lactate species. [26] Note that the integrated peak area centered at 2972 cm^{-1} detected over Na_2HPO_4/NaY-*20.1* is smaller than that detected over Na_2HPO_4/NaY_{com}. According to the FTIR results, the amount of sodium lactate in Na_2HPO_4/NaY-*n* is greater than that in Na_2HPO_4/NaY_{com}; on the other hand, the XPS results indicate similar carbon content in the two samples. On both catalysts, besides the sodium lactate, there are other species generated, such as poly-lactic acid and even inactive carbon. The XPS results imply that there should be relatively higher fraction of sodium lactate species in Na_2HPO_4/NaY-*n* while higher fraction of poly-lactic acid and inactive carbon species in Na_2HPO_4/NaY_{com}.

Our previous study [26] indicated that the deposition of poly-lactate species on the catalyst surface could cause catalyst deactivation. Therefore, the IR results infer that compared to Na_2HPO_4/NaY_{com}, the Na_2HPO_4/NaY-*n* catalysts could be more durable for the target reaction since poly-lactate and inactive carbon species in higher amount are deposited over Na_2HPO_4/NaY_{com}.

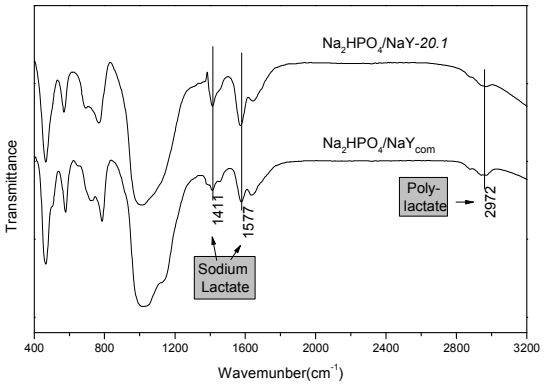

Fig 7. FTIR spectra of the used 12%Na_2HPO_4/NaY-20.1 and 12%Na_2HPO_4/NaY_{com}.

3.5 Catalyst durability

The conversion and yield as a function of time on stream over Na_2HPO_4/NaY-*26.3* as well as Na_2HPO_4/NaY_{com} have been investigated and the results are supplemented in Electronic Supplementary Information (Fig. S2, ESI). Although both

catalysts were found to deactivate with time, there is noteworthy difference between the two. According to the data shown in Fig. S2a (ESI), the decline in conversion over Na_2HPO_4/NaY-*26.3* is noticeably less than that over Na_2HPO_4/NaY_{com}. Similar trend was observed over the regenerated catalysts. It was found that there is notable decrease in AA yield at the early stage of reaction, but AA yield is essentially retained over Na_2HPO_4/NaY-*26.3* after 1000 min while it decreases continuously over Na_2HPO_4/NaY_{com} within the whole test period (Fig. S2b). According to Fig. S2b (ESI), the activity of used Na_2HPO_4/NaY-*26.3* (after 1700 min reaction) can be fully recovered through a thermo-treatment at 400°C in air. Moreover, in terms of AA yields, the regenerated catalysts deactivate more slowly as compared to the fresh ones. Na_2HPO_4/NaY-*26.3* showed better overall stability than Na_2HPO_4/NaY_{com} within the test period. The results of durability and regeneration tests suggest that the catalyst crystals are rather stable under the conditions of dehydration reaction, and this conclusion is also supported by the XRD investigation of fresh and used Na_2HPO_4/NaY-*26.3* of the same amount (Fig. S3, ESI), the used catalyst essentially retains the FAU zeolite structure after reaction. Note that the S_{BET} of the used Na_2HPO_4/NaY-*26.3* is decreased to 25.8 m^2/g, and the measured V_{micro} becomes negligible, suggesting that there is severe carbon deposition inside the micropores (after 1700-min reaction), and only the remaining external surfaces have major contribution to the catalytic reaction. Note also that the deposited inactive carbon species can be readily burn away via a thermo-treatment at 400°C in air and the zeolite porosity of used catalyst is essentially regenerated, which enables efficient activity recover over the air-treated catalyst.

In terms of the XPS results, the surface P concentration of catalysts did not decrease after reaction, which suggested that the dropped AA yield is not caused by P loss but rather the formation of poly-lactic acid and inactive carbon species. It deserves to further improve catalyst durability by elemental doping and/or higher concentration of polymerization inhibitor used in the feed to suppress formation of poly-lactate species and to hinder deposition of inactive carbon on catalyst surface.

4. Conclusion

In the present study, NaY-*n* (H_2O/SiO_2 molar ratio n = 13.8, 16.9, 20.1, 26.3) different in particle size were synthesized and used to disperse Na_2HPO_4. The commercially available NaY_{com} was adopted and treated in a similar manner as a reference. The catalysts were applied for LA dehydration to AA. Through the optimization of Na_2HPO_4 loading (12 wt%) and particle size of NaY (NaY-*20.1*), an AA yield of 74.3% can be achieved at 340°C, giving the corresponding AA formation rate of 12.0 mmol g_{cat}^{-1} h^{-1}, the highest one ever reported for LA dehydration to AA. In addition to improved catalyst durability, the new catalyst showed 17% increase in AA yield compared to the catalyst systems previously reported by us. The results of XRD investigation revealed that zeolite phase purity and texture of NaY-*n* was enhanced with increasing *n* values, and the NaY-*n* loaded with Na_2HPO_4 showed FAU structure that was only slightly distorted. Employing slightly low Si/Al ratio in NaY-*n* can modify catalyst acidity, while the pre-applied Na^+ ion-exchange and the following Na_2HPO_4 loading can effectively reduce the number of acid sites, particularly the Brønsted ones on NaY-*n*. Equrally important structural features of NaY-*n* are their shorter pore channels (or even incompletely developed zeolite texture) and relatively larger $S_{external}/S_{BET}$ ratio, which favors quick product departure from catalyst surface, and reduces the possiblity of side reactions occuring inside the long channels. In addition, higher surface concentration of Na^+ on Na_2HPO_4/NaY-*n* favors sodium lactate meanwhile suppresses poly-lactate as well as inactive carbon formation, which corresponds to the superior performance as well as improved durability of Na_2HPO_4/NaY-*n*.

Notes and references

[a] *Key Laboratory of Mesoscopic Chemistry, MOE, School of Chemistry and Chemical Engineering, Nanjing University, 22 Hankou Road, Nanjing 210093, China. Fax: +86-25-83317761; Tel: +86-25-83686270; E-mail: jiwj@nju.edu.cn*

[b] *Department of Chemistry, Hong Kong Baptist University, Kowloon Tong, Hong Kong, China, Fax: +852-34117348; E-mail: pctau@hkbu.edu.hk*

† Electronic Supplementary Information (ESI) available. See DOI: 10.1039/b000000x/

1 (a) M. Jarvinen, L. Myllykoski, R. Keiski and J. Sohlo, *Bioseparation*, 2000, **9**, 163; (b) J.M.K. Timmer, J. Kromkamp and T. Robbertsen, *J. Membr. Sci.*, 1994, **92**, 185; (c) S. Tejayadi and M. Cheryan, *Appl. Microbiol. Biotechnol.*, 1995, **43**, 242.

2 A.J.J. Straathof, S. Sie, T.T. Franco and L.A.M. Vander Wielen, *Appl. Biochem. Biotechnol*., 2005, **67**, 727.

3 X.B. Xu, J.P. Lin and P.L. Cen, *Chin. J. Chem. Eng.*, 2006, **14**, 419.

4 R. Datta and M. Henry, *J. Chem. Technol. Biot.*, 2006, **81**, 1119.

5 (a) Buehta, K. Laetieacid, H. Dellweg(ed.), *Biotechnology*, vol.3, Verlag-Chemie, Weinheim, 1983, pp. 409-417; (b) V. Shah, N. Garg, and D. Madamwar, *Appl. Biochem. Biotechnol.*, 2006, **128,** 171.

6 R.P. John, K.M. Nampoothiri, A. Pandey, *Appl. Microbiol. Biotechnol.,* 2007, **74,** 524.

7 M. Dusselier, P.V. Wouwe, A. Dewaele, E. Makshina and B.F. Sels, *Energy & Environ. Sci.*, 2013, 6, 1415.

8 (a) P. N. R. Vennestrøm, C. M. Osmundsen, C. H. Christensen, and E. Taarning, *Angew. Chem. Int. Ed.*, 2011, **50**, 10502. (b) M.S. Holm, S. Saravanamurugan, E. Taarning, Science, 2010, **328**, 602; (c) E. Taarning, S. Saravanamurugan, M.S. Holm, J. Xiong, R.M. West, C.H. Christensen, *ChemSusChem,* 2009, **2**, 625; (d) E. Taarning, C. M. Osmundsen, X. Yang, B. Voss, S. I. Andersen, C. H. Christensen, Energy. Environ. Sci., 2011, **4**, 793; (e) A. Onda, T. Ochi, K. Kajiyoshi, K. Yanagisawa, *Appl. Catal. A: Gen.*, 2008, **343**, 49. (f) P. Y. Dapsens, C. Mondelli, J. Pérez-Ramírez, ACS Catal., 2012, **2**, 1487.

9 R.E. Holmen, *US Patent*, 2859240 (1958).

10 C. Paparizos, S.R. Dolhyj and W.G. Shaw, *US Patent*, 4786756 (1988).

11 R.A. Sawicki, *US Patent*, 4729978 (1988).

12 (a) G.C. Gunter, D. J. Miller and J. E. Jackson, *J. Catal.*, 1994, **148**, 252; (b) G.C. Gunter, R.H. Langford, J.E. Jackson and D.J. Miller, *Ind. Eng. Chem. Res.*, 1995, **34**, 974; (c) G.C. Gunter, R. Craciun, M.S. Tam, J.E. Jackson and D.J. Miller, *J. Catal.*, 1996, **164**, 207; (d) M.S. Tam, G.C. Gunter, R. Craciun, D.J. Miller and J.E. Jackson, *Ind. Eng. Chem. Res.*, 1997, **36**, 3505.

13 H. Monma, *J. Catal.*, 1982, **75**, 200.

14 C. Daniel, *US Patent*, 4410729 (1983).

15 W.C. Watkins, *US Patent*, 3917673 (1975).

16 J.M. Lee, D.W. Hwang, Y. K. Hwang, S. B. Halligudi, J.S. Chang and Y.H. Han. *Catal. Comm*., 2010, **11**, 1176.

17 (a) V.C. Ghantani, S.T. Lomate, M.K. Dongare and S.B. Umbarkar, *Green Chem*., 2013, **15**,1211; (b) J.S. Peng, X.L. Li, C.M. Tang and W. Bai, *Green Chem*. 2013, DOI: 10.1039/c3gc42028k

18 Z.Q. Zhang, Y.X. Qu, S. Wang and J.D. Wang, *Ind. Eng. Chem. Res.*, 2009, **48**, 9083.

19 C.P. Lira and P.J. McCrackin, *Ind. Eng. Chem. Res.*, 1993, **32**, 2608.
20 C.Park and M.A. Keane, *J. Mol. Catal. A: Chem.*, 2001, **166**, 303.
21 R.P.K. Wells, P. Tynj l , J.E. Bailie, D.J. Willock, G.W. Watson, F. King, C.H. Rochester, D. Bethell, P.C. Bulman Page and G.J. Hutchings, *Appl. Catal. A.,* 1999, **182**, 75.
22 J.F. Zhang, X.Z. Feng, Y.L. Zhao, W.J. Ji, and C.-T. Au, *J. Ind. Eng. Chem.* 2013, http://dx.doi.org/10.1016/j.jiec.2013.07.018
23 K.J. Balkus and A.K. Khanmamedova, *J. Catal.,* 1995, **151**, 10.
24 H.J. Wang, D.H. Yu, P. Sun, J. Yan, Y. Wang, H. Huang, *Catal. Comm.*, 2008, **9**, 1799.
25 (a) P. Sun, D.H. Yu, K. Fu, M. Gu, Y. Wang, H. Huang and H. Ying, Catal. Comm., 2009, **10**, 1345; (b) P. Sun, D.H. Yu, Z.C. Tang, H. Li and H. Huang, *Ind. Eng. Chem. Res.,* 2010, **49**, 9082.
26 J.F. Zhang, Y.L. Zhao, M. Pan, X.Z. Feng, W.J. Ji and C.T. Au, *ACS Catal.,* 2011, **1**, 32.
27 Y. Huang, K. Wang, D.H. Dong, D. Li, M.R. Hill, A.J. Hill, and H. Wang, *Micropor. Mesopor. Mater.*, 2010, **127**, 167.
28 W.G. Song, G.H. Li, V.H. Grassian and S.C. Larsen, *Environ. Sci. Technol.*, 2005, **39**, 1214.
29 P. Samaras, X. Dabou, G.P. Sakellaropoulos, Studies in Surface Science and Catalysis, 123: Catalysis-an Integrated Approach, (Eds: R.A.van Santen, P. van Leeuwen, J.A. Moulijn, B.A. Averill), Elsevier, Amsterdam, The Netherlands, 1999, pp. 543.
30 J. Rouquerol, P. Llewellyn and F. Rouquerol, *Studies in Surface Science and Catalysis,* **167**: Characterization of Porous Solids VII, (Eds: P.L. Llewellyn, F. Rodriquez-Reinoso, J. Rouqerol, N. Seaton), Elsevier, Amsterdam, The Netherlands, 2007, pp. 49.
31 A. Jentys and J.A. Lercher, *Studies in Surface Science and Catalysis*, **137**: Introduction to Zeolite Science and Practice, (Eds: H. van Bekkum, E.M. Flanigen, P.A. Jacobes, J.C. Jansen), Elsevier, Amsterdam, The Netherlands, 2001, pp. 345.
32 F. Benaliouche, Y. Boucheffa, P. Ayrault, S. Mignard and P. Magnoux, *Micropor. Mesopor. Mater.*, 2008, **111**, 80.
33 R.B. Borade and A. Clearfield, J. Mol. Catal., 1994, **88**, 249.
34 Q. Xin and M.F. Luo (Eds), *Modern Characterization Techniques in Catalysis*, Science and Technology Press, Beijing, 2009, pp.142.
35 Y.M. Fang, H.Q. Hu and G.H. Chen, *Chem. Mater.*, 2008, **20**, 1670.
36 S.Y. Sang, Z.M. Liu, P. Tian, L.H. Qu and Y.Y. Zhang, *Mater. Lett.*, 2006, **60**, 1131.
37 V.P. Valtchev, and K.N. Bozhilov, *J. Phys. Chem. B*, 2004, **108**, 15587.
38 J. F. Zhang, J. P. Lin and P. Cen, *Cana. J. Chem. Eng.*, 2008, **86**, 1047.

Table of Contents

Na_2HPO_4-modified NaY nanocrystallites: Efficient catalyst for acrylic acid production through lactic acid dehydration

Junfeng Zhang, Yuling Zhao, Xinzhen Feng, Min Pan, Jing Zhao, Weijie Ji,* and Chek-Tong Au*

Acrylic acid yield of 74.3% has been achieved at 340°C in lactic acid dehydration over Na_2HPO_4-modified NaY nanocrystallites (NaY-*n*), giving acrylic acid formation rate of 12.0 mmol g_{cat}^{-1} h^{-1}. Appropriate surface acidity together with unique structural feature of NaY-*n* ensures efficient lactic acid conversion with high acrylic acid selectivity.